

Stability and Dynamic of HIV-1 Mathematical Model with Logistic Target Cell Growth, Treatment Rate, Cure Rate and Cell-to-cell Spread

Najmeh Akbari*, Rasoul Asheghi and Maryam Nasirian

Abstract. One way of HIV infection spreading is through the cell division of infected cells by mitosis expressed in mathematical models as a logistic process. Cell-to-cell transmission is another factor in the spread and speed of disease. In this work, we present a five-dimensional Ordinary Differential Equation model (ODE) with the logistic form for proliferation of uninfected cells, cell-to-cell and virus-to-cell transmission rate, two types of cellular and humoral immune responses, the cure rate for returning infected cells to non-infectious cells, and two treatment rates, one for reducing infectious cells and the other for blocking free viruses. We discuss the positivity and boundedness of solutions, free-equilibrium points, steady-state equilibrium points, and stability by the Routh Hurwitz criterion. The rate of reproduction is analyzed, and the useful parameters for increasing or decreasing it are identified. Numerical simulations are performed to investigate the dynamic behavior of model responses to treatment effects on disease.

1. Introduction

AIDS, acquired immune deficiency syndrome, was first reported in the United States in 1981 by the Centers for Disease Control and Prevention. AIDS is a syndrome caused by a retrovirus, Human Immunodeficiency Virus. The disease involves severe weakness of the immune system that, by arrival, opportunistic infections in the body, eventually resulting in death. AIDS is recognized as a global epidemic disease [14].

HIV is a lentivirus from the family of retroviruses. There are two types of HIV viruses: HIV-1 and HIV-2. Most of the registered cases are HIV-1. HIV is a virus that attacks components of the immune system such as lymphocyte cells with the CD_4^+ receptor, macrophages, and dendritic cells [3]. It should be noted that the interval between the entry of the virus into the body and the time of diagnosis by the laboratory (sufficient amount of antibody secreted in the blood) is the window period. It usually lasts about 2 to 12 weeks, but maybe longer if you have an autoimmune disease or hepatitis B. If the

Received May 29, 2021; Accepted November 15, 2021.

Communicated by Je-Chiang Tsai.

2020 *Mathematics Subject Classification.* 34A34, 34C11, 34D20.

Key words and phrases. HIV mathematical model, logistic growth, treatment rate, cure rate, cell-to-cell transmission, stability.

*Corresponding author.

affected person receives no treatment at the latency stage, and the CD_4^+ cell count declines over time to less than 200 cells per microliter, the person will enter stage AIDS. At this stage, following the severe weakening of the immune system, opportunistic infections are activated in the body and eventually lead to patient death [1].

Mathematical modeling is the attempt to present a mathematical model for a system that applies not only to the natural sciences such as physics, biology, geology, meteorology, engineering sciences, computer science, and artificial intelligence, but also to the social sciences such as economics, psychology, sociology, and medicine. Mathematical modeling helps researchers that analyze a system and predict its behavior. The process of describing a system (e.g., disease spread) requires assumptions, access to data to estimate values of the model parameters, quantitative or qualitative predictions, and comparison of results with observational or experimental data. So the crucial role of mathematical models is to help understand a system. Besides, mathematical models can help understand the importance of interventions in disease control and predict the disease's future status. However, it is essential to understand the limitations of a model, the uncertainty in the parameter values, the model's non-linearity, and chance events in the model [15]. In recent decades, several intracellular dynamic models have been defined for the HIV-1 virus. These models describe the reaction between the virus and the host cells in diseased individuals and are valuable for understanding the dynamics of viral infections and the effectiveness of viral therapy [38].

The first HIV models at the late 1980 are expressed immediately after the discovery of the HIV, by Merrill [26] in 1987, Anderson and May in 1989 [4]. In 1989, Perelson proposed a model explaining many of the HIV infection's immunological consequences. In this model, the cell proliferation rate of CD_4^+ T is logically expressed. Note that the logistic law is based on the fact that the growth of T cells (or any normal cell) stops as their population approaches T_{\max} . The term logistical growth here refers to the growth of T cells' population in the vicinity of a viral infection. One assumption of logistic growth of T cells is that if $T(0) < T_{\max}$, for all t then $T(t) < T_{\max}$. Thus, when the T cell population reaches its maximum, the presence of HIV will infect these cells [22, 28].

In 1993, Perelson et al. studied a model dynamics that showed the effects of AZT antiviral drugs that inhibited the Reverse Transcription enzyme to prevent virus replication [30]. In 1996, Nowak and Bangam presented a simple model for antiviral immune response, virus replication, and virus diversity. They proposed three models. In the first model, a simple interaction between virus replication and host cells was demonstrated. Since the immune responses reduce viral load, the second model included immune responses against infected cells and, finally, a model in which the virus can reproduce and evade the immune responses that are the result of an HIV mutation [27]. In 1997, Kirschner

et al. proposed a model used to simulate HIV infection chemotherapy. In this simulation, antiviral drugs are including Reverse Transcription and Protease Inhibitors. In this model, drug-resistant and susceptible viral strains have been shown to play an essential role in the efficacy of HIV chemotherapy [21]. In 2007, Wodarz et al. used two cell types of CD_4^+ T cells and macrophages in their model and suggested that infected CD_4^+ T cells could stimulate by antigens and then divide. Then they expressed this rate as a logistic function [37]. In 2009, Martin et al. argued that cell-to-cell transmission is a more robust and more sensitive mechanism than the mechanism of virus-to-cell infection. Cell-to-cell proliferation not only simplifies the rapid spread of the virus but also reduces the effect of antibodies for viral Inhibitors by evading immune attacks [25]. In 2010, Gang Huang examined a set of differential equations with non-linear infection transmission rates. In this model, to provide a more complex and general infection process, the contact rate between the target cells and the virus non-linear is considered [18]. In 2011, Sigal et al. stated that cell-to-cell expansion of HIV-1 reduces the efficacy of antiviral treatment because cell-to-cell transmission can cause many infections in target cells, which can reduce the sensitivity to antiviral drugs [31]. In 2011, Xu states the model in which the saturation collision rate is used instead of the linear collision rate for virus and cell contact [39]. In 2012, Yan and Wang described a model that included both cell-mediated and humoral immune responses and involved only the process of virus-to-cell infection [40]. In 2013, Wang et al. presented an HIV model that included CTL immune response and antiviral treatment. In this model, CD_4^+ T cell proliferation in the presence of the virus is expressed as a logistic function [36]. At 2015, Foutz et al. Stated the principle of HIV vaccine design based on the combined efficacy of cellular and humoral immunity [13]. In 2016, Kamboj announced a model of Reverse Transcription and Protease Inhibitors drug therapy with the proliferation rate of logistic [19]. In 2017, Alawi et al. replaced the saturation function $\frac{\beta_1 v(t)}{1+\alpha v(t)}$ instead of the bilinear infection rate [10]. In 2018, Lin et al. proposed an HIV-1 model with virus-to-cell infection, cell-to-cell infection, cellular and humoral immune response, and saturation incidence rate of the virus are considered [23].

When a virus enters a CD_4^+ T cell, several biological Processes can occur: the reverse transcription of the viral RNA to DNA, binding of DNA to the infected cell DNA (called provirus), transcription of the provirus, and translation to make viral polypeptides, fragmentation of polypeptides by HIV protease, and germination of new viruses [30]. After entering viruses into resting CD_4^+ T cells, the reverse transcription of the cell is completed if the cell is activated. But, if viral RNA is not completely transcribed into DNA, then the integrated virus stored in the resting CD_4^+ T cells may die out over time. So, the reverse transcription of DNA becomes unstable and can be quickly degraded. Thus, a proportion of resting infected CD_4^+ T cells can be reverted to the uninfected cells [11,42,43]. Authors

of [29] state that when a virus enters a CD_4^+ T, chemotherapy can affect it, and this can change some infected cells into uninfected ones. Moreover, the current combination of antiretroviral therapies, including the Reverse Transcription and Protease Inhibitors, can restore some infected CD_4^+ T cells to uninfected ones, by losing all cccDNA from their nuclei [5]. In 2016, Kaminski developed a method for curing infected cells by gene therapy or loss of all cccDNA from their nucleus [20]. With the above hypotheses, in the papers [2, 7, 41], the reversibility process of a part of infected cells to uninfected cells is considered with one parameter.

The mathematical model seems more realistic when all the factors contributing to the spread of the disease are expressed in it. However, since the dynamic study of a mathematical model with many variables and parameters is difficult and practically impossible, in most of the above models, for a simpler study of its dynamics, some existing factors are assumed to be constant and not included in the model. The innovation of this model is that with adding several factors from different papers such as cure rate, the proliferation rate of healthy cells with logistic function, the infection rate of healthy cells non-linearly, the spread of infection through cell-to-cell and virus-to-cell process, and cellular and humoral immunity, dynamics are examined.

The paper is organized as follows. In Section 2, we formulate a model with five state variables. In Section 3, we study the non-negative and boundedness of solutions. In Section 4, we analyze infection-free equilibrium points. In Section 5, we investigate steady-state equilibrium points. In Section 6, we examine the role of parameters in the rate of reproduction. In Section 7, we consider the numerical simulation of the model (2.1). In the last section, we conclude.

2. Model formulation

The population of CD_4^+ T cells is stimulated by antigens and then divided. Therefore, when their community reaches its maximum, their reproduction stops. Hence, their reproduction rate can be expressed as a logistic function. Also, to make a realistic model, the saturation function was used instead of the bilinear infection rate. On the other hand, because cell-to-cell transmission of the virus plays an essential role in reducing antibodies effect on viral Inhibitors, it has been considered along with virus-to-cell transmission. Also, due to antiviral drugs effectiveness in HIV chemotherapy's success, their effect is examined in the model. Then, both cellular and humoral immune systems have been used together for the effectiveness of the principle of Foutz vaccine design. Besides, Kaminsky gene therapy has been used to cure infected cells. A cure rate is stated as a method for averting of infected cells to uninfected cells by gene therapy or loss of all cccDNA from their nucleus.

Parameters	Description
r	The rate at which the CD_4^+ T-cells are reproduced.
m	Maximum value of CD_4^+ T-cells in the absence of the virus.
β_1	The rate at which the virus infects the CD_4^+ T-cells.
β_2	The rate at which the CD_4^+ T-cells are infected by the infected cells.
α	The rate at which the viruses are saturated.
ρ	The cure rate of the infected CD_4^+ T-cells that reverted to the uninfected T-cells.
d	The death rate of the CD_4^+ T-cells.
δ	The death rate of the infected CD_4^+ T-cells.
ρ_1	The rate at which the T-cells kill the infected CD_4^+ T-cells.
η	The treatment rate at which measure the efficacy of Reverse Transcriptase Inhibitor.
ε	The treatment rate at which measure the efficacy of protease Inhibitor.
n	Number of viruses produced by the infected CD_4^+ T-cells.
μ	The death rate of the viruses.
ρ_2	The rate at which the B-cells kill the viruses.
c_1	The rate at which the presence of the infected T-cells activates the T-cells.
b_1	The death rate of the T-cells.
c_2	The rate at which the presence of the virus activates the B-cells.
b_2	The death rate of the B-cells.

Table 2.1: Used parameters in HIV mathematical model.

Now, we extend a mathematical model for HIV infection with two treatment rates, cure rate, the transmission of infection by the virus-to-cell and cell-to-cell, logistic growth for CD_4^+ T-cell uninfected, the saturation function for the infection rate, and both types of cellular and humoral immune systems. We use five state variables in the model. Population of uninfected CD_4^+ T-cells (x), Population of infected CD_4^+ T-cells (y), Population of infectious HIV virions (v), Population of T-cells (z), Population of B-cells (w). Also, two parameters $\eta, \varepsilon \in [0, 1]$ have been introduced as treatment rates of Reverse Transcriptase Inhibitors (RTIs) and Protease Inhibitors (PIs) respectively. Reverse Transcriptase Inhibitor prevents the transcriptase process in cells infected by the virus HIV, and Protease Inhibitor blocks the protease enzyme, thereby preventing the production of infectious and mature viruses. The proposed model is illustrated below.

$$\begin{aligned}
 \frac{dx}{dt} &= rx \left(1 - \frac{x+y}{m} \right) - \frac{(1-\eta)\beta_1 vx}{1+\alpha v} - \beta_2 xy + \rho y - dx, \\
 \frac{dy}{dt} &= \frac{(1-\eta)\beta_1 vx}{1+\alpha v} + \beta_2 xy - (\delta + \rho)y - \rho_1 yz, \\
 \frac{dv}{dt} &= (1-\varepsilon)n\delta y - \mu v - \rho_2 vw, \quad \frac{dz}{dt} = c_1 yz - b_1 z, \quad \frac{dw}{dt} = c_2 vw - b_2 w.
 \end{aligned}
 \tag{2.1}$$

All parameters in model (2.1) are positive and assumed to be independent of time. They are described in Table 2.1.

3. Non-negative and boundedness of solutions

For biological reasons, we suppose that the initial values of the variables of the system (2.1) are non-negative. Then, we prove that all of its solutions are also non-negative and bounded.

Proposition 3.1. *Let $\Gamma(t) = (x(t), y(t), v(t), z(t), w(t))$, with $x(0) \geq 0, y(0) \geq 0, v(0) \geq 0, z(0) \geq 0, w(0) \geq 0$, be a solution of the system (2.1). Then $0 \leq x(t) \leq M, 0 \leq y(t) \leq M, 0 \leq v(t) \leq M, 0 \leq z(t) \leq M, 0 \leq w(t) \leq M$ for all $t \geq 0$, for some $M > 0$.*

Proof. We know that $\Gamma(t)$ is the solution of system (2.1) with the initial values

$$\{x(0) \geq 0, y(0) \geq 0, v(0) \geq 0, z(0) \geq 0, w(0) \geq 0\}.$$

Then

$$\dot{x}|_{x=0} = \rho y \geq 0, \quad \dot{y}|_{y=0} = \frac{\eta_1 v x}{1 + \alpha v} \geq 0, \quad \dot{v}|_{v=0} = \delta_1 y \geq 0, \quad \dot{z}|_{z=0} = 0, \quad \dot{w}|_{w=0} = 0.$$

The above computations show that the solutions of system (2.1) so long as $y(x) > 0$ with non-negative initial values remain in the first quadrant for all $t \geq 0$, and hence, they are non-negative. Now we prove the boundedness property. To this end, we set $T = x + y$ with $x, y \geq 0$, and from the sum of the first two equations of (2.1), we get

$$\dot{T} = \dot{x} + \dot{y} = rx \left(1 - \frac{x + y}{m}\right) - \delta y - dx - \rho_1 yz.$$

It is clear that when $x + y \geq m$, we have $\dot{T} < 0$, and so, T is decreasing, and hence it is bounded. This implies that the functions x and y are bounded on $[0, \infty)$. From the third equation of system (2.1), we have

$$\dot{v} = \delta_1 y - \mu v - \rho_2 v w \leq \delta_1 y - \mu v,$$

which by integrating gives

$$v(t) \leq v(0)e^{-\mu t} + \delta_1 \int_0^t y(s)e^{-\mu(t-s)} ds.$$

Noting that the function y is bounded on $[0, \infty)$, we can assume that $|y(s)| \leq K_1$ for some $K_1 > 0$, and hence

$$v(t) \leq v(0) + \frac{\delta_1 K_1}{\mu}(1 - e^{-\mu t}) \leq v(0) + \frac{\delta_1 K_1}{\mu} \quad \text{for all } t \geq 0.$$

From the fourth equation, $\dot{z} = c_1 yz - b_1 z$, and by using the first and second equations of (2.1), we have

$$\begin{aligned} \dot{z} + b_1 z &= c_1 yz = \frac{c_1}{\rho_1} \left\{ rx \left(1 - \frac{x+y}{m} \right) - (\dot{x} + dx) - (\dot{y} + \delta y) \right\} \\ &\leq \frac{c_1}{\rho_1} \{(r-d)x - \delta y - \dot{x} - \dot{y}\}. \end{aligned}$$

Therefore,

$$\begin{aligned} z(t) &\leq e^{-b_1 t} \left\{ z(0) + \frac{c_1}{\rho_1} (x(0) + y(0)) \right\} - \frac{c_1}{\rho_1} (x(t) + y(t)) \\ &\quad + \frac{c_1}{\rho_1} \left\{ \int_0^t ((r-d+b_1)x(s) + (b_1-\delta)y(s)) e^{-b_1(t-s)} ds \right\}. \end{aligned}$$

Now we consider the following cases:

(a) If $(r-d+b_1) \leq 0$ and $(b_1-\delta) \leq 0$, then

$$z(t) \leq z(0) + \frac{c_1}{\rho_1} [x(0) + y(0)].$$

(b) If $(r-d+b_1) \leq 0$ and $(b_1-\delta) > 0$, then due to the fact that $y(s)$ is bounded on $[0, \infty)$ so that $|y(s)| \leq K_1$, we have

$$z(t) \leq z(0) + \frac{c_1}{\rho_1} \left[x(0) + y(0) + K_1 \left(1 - \frac{\delta}{b_1} \right) \right].$$

(c) If $(r-d+b_1) \geq 0$ and $(b_1-\delta) \leq 0$, then by using that $x(s)$ is bounded on $[0, \infty)$, we take $|x(s)| \leq K_2$ and we get

$$z(t) \leq z(0) + \frac{c_1}{\rho_1} \left[x(0) + y(0) + K_2 \left(1 + \frac{r-d}{b_1} \right) \right].$$

(d) If $(r-d+b_1) \geq 0$ and $(b_1-\delta) \geq 0$, then

$$z(t) \leq z(0) + \frac{c_1}{\rho_1} \left[x(0) + y(0) + K_1 \left(1 + \frac{\delta}{b_1} \right) + K_2 \left(1 + \frac{r-d}{b_1} \right) \right].$$

The equations $\dot{w} = c_2 vw - b_2 w$ and $\dot{v} = \delta_1 y - \mu v - \rho_2 vw$ imply that

$$\dot{w} + b_2 w = c_2 vw = \frac{c_2}{\rho_2} \{\delta_1 y - (\dot{v} + \mu v)\}.$$

By integrating, we obtain that

$$w(t) \leq e^{-b_2 t} \left\{ w(0) + \frac{c_2}{\rho_2} v(0) \right\} + \frac{c_2}{\rho_2} \left\{ \int_0^t [\delta_1 y(s) + (b_2 - \mu)v(s)] e^{-b_2(t-s)} ds \right\}.$$

Now we consider the following:

(a) If $b_2 - \mu \leq 0$, then $w(t) \leq w(0) + \frac{c_2}{\rho_2} [v(0) + \frac{\delta_1}{b_2} K_1]$.

(b) If $b_2 - \mu \geq 0$, then by the boundedness of v , we assume $|v| \leq K_3$ and we get $w(t) \leq w(0) + \frac{c_2}{\rho_2} [v(0) + \frac{\delta_1}{b_2} K_1 + (1 - \frac{\mu}{b_2}) K_3]$.

Putting all together with the above calculations, we conclude that all the solutions of system (2.1) are bounded. □

4. Infection-free equilibrium points

In this section, we study the conditions of existence and stability of the infection-free equilibrium points of the system (2.1), and we compute the basic reproduction number associated with them. According to [6], the basic reproduction number indicates the number of secondary infections by an infectious cell during proliferation. In the HIV model, the basic reproduction number plays an important role in spreading the reproduction of infection among healthy CD_4^+ T-cells. System (2.1) has two infection-free equilibrium points $E_{00} = (0, 0, 0, 0, 0)$ and $E_{01} = (\frac{m(r-d)}{r}, 0, 0, 0, 0)$. At E_{01} , the uninfected CD_4^+ cells reach to the maximal level. In this case, the disease cannot raid.

4.1. Local stability of the infection-free equilibrium points

We suppose \mathcal{R}_0 is the basic reproduction number of system (2.1) for the infection-free equilibrium point E_{00} that is given by $\mathcal{R}_0 = \frac{r}{d}$.

Proposition 4.1. *If $\mathcal{R}_0 = \frac{r}{d} < 1$, then the infection-free equilibrium point $E_{00} = (0, 0, 0, 0, 0)$ of system (2.1) is asymptotically stable and it is unstable when $\mathcal{R}_0 > 1$.*

Proof. The Jacobian matrix of system (2.1) at $E_{00} = (0, 0, 0, 0, 0)$ is given by

$$J_{E_{00}} = \begin{bmatrix} r - d & \rho & 0 & 0 & 0 \\ 0 & -(\delta + \rho) & 0 & 0 & 0 \\ 0 & \delta_1 & -\mu & 0 & 0 \\ 0 & 0 & 0 & -b_1 & 0 \\ 0 & 0 & 0 & 0 & -b_2 \end{bmatrix}.$$

It is obvious that, the eigenvalues of the matrix $J_{E_{00}}$ are

$$\lambda_1 = r - d, \quad \lambda_2 = -(\delta + \rho) < 0, \quad \lambda_3 = -\mu < 0, \quad \lambda_4 = -b_1 < 0, \quad \lambda_5 = -b_2 < 0.$$

Now it is clear that for $\mathcal{R}_0 < 1$, all the eigenvalues of the Jacobian matrix $J_{E_{00}}$ are negative, and hence, the free-equilibrium point E_{00} is locally asymptotically stable, and it is unstable for $\mathcal{R}_0 > 1$. □

By a simple calculation, we can show that the basic reproduction number of system (2.1) for the infection-free equilibrium point E_{01} is given by

$$(4.1) \quad \mathcal{R}_1 = \frac{m(r-d)(\eta_1+B)}{rA},$$

where $\eta_1 = (1-\eta)\beta_1$, $A = \frac{\mu(\delta+\rho)}{\delta_1}$, $B = \frac{\beta_2\mu}{\delta_1}$, and $\delta_1 = (1-\varepsilon)n\delta$. The threshold number \mathcal{R}_1 denotes the number of infectious cells produced by the proliferation of an infectious cell [9].

Theorem 4.2. *The disease-free equilibrium point E_{01} is asymptotically stable when $0 < \mathcal{R}_1 < 1$ and it is unstable when $\mathcal{R}_1 > 1$.*

Proof. To simplify the calculations, we set $A = \frac{\mu(\delta+\rho)}{\delta_1}$ and $B = \frac{\mu\beta_2}{\delta_1}$. Then, the Jacobian matrix of system (2.1) at the disease-free equilibrium point E_{01} is given by

$$J_{E_{01}} = \begin{bmatrix} d-r & \frac{1}{r}(r\rho+(d-r)(r+\beta_2m)) & \frac{\eta_1m}{r}(d-r) & 0 & 0 \\ 0 & \frac{\beta_2m}{r}(r-d)-(\delta+\rho) & -\frac{\eta_1m}{r}(d-r) & 0 & 0 \\ 0 & \delta_1 & -\mu & 0 & 0 \\ 0 & 0 & 0 & -b_1 & 0 \\ 0 & 0 & 0 & 0 & -b_2 \end{bmatrix}.$$

The characteristic polynomial of $J_{E_{01}}$ is equal to

$$P_{J_{E_{01}}}(\lambda) = (d-r-\lambda)(-b_1-\lambda)(-b_2-\lambda)(\lambda^2+a_1\lambda+a_2).$$

Thus, the eigenvalues of the Jacobian matrix $J_{E_{01}}$ are

$$\begin{aligned} \lambda_1 &= d-r < 0, & \lambda_2 &= -b_1 < 0, & \lambda_3 &= -b_2 < 0, \\ \lambda_4 &= \frac{-a_1 + \sqrt{a_1^2 - 4a_2}}{2} < 0, & \lambda_5 &= \frac{-a_1 - \sqrt{a_1^2 - 4a_2}}{2} < 0, \end{aligned}$$

where

$$\begin{aligned} a_1 &= (\delta+\rho+\mu) - \frac{\beta_2m}{r}(r-d), \\ a_2 &= \mu(\delta+\rho) - \frac{\mu m\beta_2}{r}(r-d) - \frac{\delta_1\eta_1m}{r}(r-d) = \delta_1 \left(A - \frac{m}{r}(r-d)(\eta_1+B) \right). \end{aligned}$$

For $0 < \mathcal{R}_1 = \frac{m(r-d)(\eta_1+B)}{rA} < 1$, we have $a_2 > 0$, which implies

$$\frac{\beta_2m}{r}(r-d) < (\delta+\rho) - \frac{\delta_1\eta_1m}{r}(r-d) < \delta+\rho < \delta+\rho+\mu.$$

The above gives $a_1 > 0$. Therefore, the eigenvalues $\lambda_1, \lambda_2, \lambda_3, \lambda_4$ and λ_5 are negative, and this shows that E_{01} is locally asymptotically stable. □

5. Steady-state equilibrium points

In this section, we discuss the conditions of existence and stability of the infection steady-state equilibrium points. All the steady-state equilibrium points exist when $\mathcal{R}_1 > 1$. It shows the presence and spread of the disease. We can show that for $\mathcal{R}_1 > 1$, system (2.1) has four equilibrium points. It has an equilibrium point $E_1 = (x_1, y_1, v_1, 0, 0)$, where

$$x_1 = \frac{A(1 + \alpha v_1)}{\eta_1 + B(1 + \alpha v_1)}, \quad y_1 = \frac{\mu}{\delta_1} v_1,$$

and v_1 is the positive real root of the equation $\psi_3 v^3 + \psi_2 v^2 + \psi_1 v + \psi_0 = 0$, for $\psi_0 < 0$, where

$$\begin{aligned} \psi_3 &= \frac{B\alpha^2\mu}{\delta_1}(rA + \delta Bm), \\ \psi_2 &= -mA\alpha^2B(r - d) + rA^2\alpha^2 + \frac{\mu r A \alpha}{\delta_1}(\eta_1 + 2B) + \frac{2\delta\mu m B \alpha}{\delta_1}(\eta_1 + B), \\ \psi_1 &= -mA\alpha(r - d)(\eta_1 + 2B) + 2rA^2\alpha + \frac{\mu r A}{\delta_1}(\eta_1 + B) + \frac{\delta\mu m}{\delta_1}(\eta_1 + B)^2, \\ \psi_0 &= -mA(r - d)(\eta_1 + B) + rA^2. \end{aligned} \tag{5.1}$$

In addition, by setting $A_2 = \frac{\delta_1}{\mu}(\eta_1 + B\alpha_2)$ and $\alpha_2 = 1 + \alpha v_2$, system (2.1) has an equilibrium point $E_2 = (x_2, y_2, v_2, z_2, 0)$, where

$$x_2 = \frac{(\delta + \rho + \rho_1 z_2)\alpha_2}{A_2}, \quad y_2 = \frac{b_1}{c_1}, \quad v_2 = \frac{\delta_1 b_1}{c_1 \mu},$$

and z_2 is the unique positive solution of the equation $T_2 z^2 + T_1 z + T_0 = 0$ for $T_0 < 0$, where

$$\begin{aligned} T_2 &= \rho_1^2 \alpha_2^2 > 0, \\ T_1 &= 2(\delta + \rho)\rho_1 \alpha_2^2 - \left(\frac{m(r - d)}{r} - \frac{b_1}{c_1}\right)\rho_1 \alpha_2 A_2 + \frac{\rho_1 m b_1 A_2^2}{rc_1}, \\ T_0 &= (\delta + \rho)^2 \alpha_2 (1 - \mathcal{R}_1) + \frac{A\delta_1 \alpha_2 b_1}{c_1 \mu} \left(\frac{A\alpha\delta_1^2}{\mu^2} + A_2\right) + \frac{\delta m b_1}{rc_1} A_2^2. \end{aligned} \tag{5.2}$$

Let $N = \frac{\rho_2}{\mu}$, $A_3 = \frac{\mu b_2}{c_2 \delta_1}$ and $\alpha_3 = 1 + \alpha v_3$. Then, system (2.1) has another equilibrium point $E_3 = (x_3, y_3, v_3, 0, w_3)$, where

$$x_3 = \frac{A(Nw_3 + 1)\alpha_3}{\eta_1 + B(Nw_3 + 1)\alpha_3}, \quad y_3 = A_3(Nw_3 + 1), \quad v_3 = \frac{b_2}{c_2},$$

and w_3 is the positive real root of the equation $Q_3w^3 + Q_2w^2 + Q_1w + Q_0 = 0$ when $Q_0 < 0$, where

$$\begin{aligned} Q_3 &= m\delta A_3 N^3 B^2 \alpha_3^2 + AA_3 BN^3 \alpha_3^2 r > 0, \\ Q_2 &= rA^2 N^2 \alpha_3^2 - m(r-d)AN^2 \alpha_3^2 B + 2rA\alpha_3^2 A_3 N^2 B + rA\alpha_3 A_3 N^2 (B\alpha_3 + \eta_1) \\ &\quad + m\delta A_3 N^2 B^2 \alpha_3^2 + 2m\delta A_3 N^2 B\alpha_3 (B\alpha_3 + \eta_1), \\ Q_1 &= 2rA^2 N \alpha_3^2 - mA\alpha_3^2 BN(r-d) - mA\alpha_3 N(r-d)(B\alpha_3 + \eta_1) + rA\alpha_3^2 A_3 BN \\ &\quad + 2rA\alpha_3 A_3 N(B\alpha_3 + \eta_1) + 2m\delta A_3 BN\alpha_3 (B\alpha_3 + \eta_1) + m\delta A_3 N(B\alpha_3 + \eta_1)^2, \\ Q_0 &= rA^2 \alpha_3^2 - mA\alpha_3 (r-d)(B\alpha_3 + \eta_1) + rA\alpha_3 A_3 (B\alpha_3 + \eta_1) + m\delta A_3 (B\alpha_3 + \eta_1)^2. \end{aligned}$$

By letting $\rho_2 = N\mu$, $N_1 = \frac{\delta_1 b_1 c_2}{\mu c_1 b_2}$, $N_2 = \frac{N_1 \mu \rho_1}{\delta_1}$ and $\alpha_4 = 1 + \alpha v_4$, we see that the fourth equilibrium point of the system (2.1) is $E_4 = (x_4, y_4, v_4, z_4, w_4)$, in which

$$x_4 = \frac{(N_1 A + N_2 z_4) \alpha_4}{\eta_1 + BN_1 \alpha_4}, \quad y_4 = \frac{b_1}{c_1}, \quad v_4 = \frac{b_2}{c_2}, \quad w_4 = \frac{N_1 - 1}{N},$$

and z_4 is the positive real root of the quadratic equation $\Psi_2 z^2 + \Psi_1 z + \Psi_0 = 0$, where

$$\begin{aligned} (5.3) \quad \Psi_2 &= rN_2^2 \alpha_4^2, \\ \Psi_1 &= 2rN_1 AN_2 \alpha_4^2 - N_2 \alpha_4 (m(r-d) - ry_4)(BN_1 \alpha_4 + \eta_1) + my_4 \rho_1 (BN_1 \alpha_4 + \eta_1)^2, \\ \Psi_0 &= rN_1^2 A^2 \alpha_4^2 - N_1 A \alpha_4 m(r-d)(BN_1 \alpha_4 + \eta_1) + ry_4 N_1 A \alpha_4 (BN_1 \alpha_4 + \eta_1) \\ &\quad + my_4 \delta (BN_1 \alpha_4 + \eta_1)^2. \end{aligned}$$

5.1. Local stability of the equilibrium points

Theorem 5.1. *The following holds:*

- (i) *If $\mathcal{R}_1 < 1$, then the equilibrium point E_1 does not exist.*
- (ii) *If $\mathcal{R}_1 = 1$, then the equilibrium point $E_1 = E_{01}$.*
- (iii) *If $\mathcal{R}_1 > 1$, then the equilibrium point E_1 exists and it is locally asymptotically stable for $v_1 < \min \left\{ \frac{b_1 \delta_1}{c_1 \mu}, \frac{b_2}{c_2} \right\}$, and it is unstable for $v_1 > \frac{b_1 \delta_1}{c_1 \mu}$ or $v_1 > \frac{b_2}{c_2}$.*

Proof. It is clear that if $\mathcal{R}_1 < 1$, then all the coefficients defined in (5.1) of the polynomial $\psi_3 v^3 + \psi_2 v^2 + \psi_1 v + \psi_0$ are positive and it has no positive roots. If $\mathcal{R}_1 = 1$, then $\psi_0 = 0$ and the only non-negative root of the polynomial $\psi_3 v^3 + \psi_2 v^2 + \psi_1 v + \psi_0$ is zero. Then $E_1 = E_{01}$. To show the existence of $E_1 = (x_1, y_1, v_1, 0, 0)$, we prove that the equation

$$\psi_3 v^3 + \psi_2 v^2 + \psi_1 v + \psi_0 = 0,$$

with $\psi_0 < 0$ has at least a positive real root. Since

$$\psi_0 = rA^2 - mA(r-d)(\eta_1 + B) = rA^2 \left(1 - \frac{m(r-d)(\eta_1 + B)}{rA} \right) = rA^2(1 - \mathcal{R}_1),$$

then $\psi_0 < 0$ when $\mathcal{R}_1 > 1$. Now we use the linearization method to determine the stability of the equilibrium point E_1 . The Jacobian matrix evaluated at the equilibrium point E_1 is given by

$$J_{E_1} = \begin{bmatrix} -\frac{rx_1}{m} - \frac{\rho y_1}{x_1} & -\frac{rx_1}{m} + \rho - \beta_2 x_1 & -\frac{\eta_1 x_1}{\alpha_1^2} & 0 & 0 \\ \frac{\eta_1 v_1}{\alpha_1} + \beta_2 y_1 & -\frac{\eta_1 \delta_1 x_1}{\alpha_1 \mu} & \frac{\eta_1 x_1}{\alpha_1^2} & -\rho_1 y_1 & 0 \\ 0 & \delta_1 & -\mu & 0 & -\rho_2 v_1 \\ 0 & 0 & 0 & c_1 y_1 - b_1 & 0 \\ 0 & 0 & 0 & 0 & c_2 v_1 - b_2 \end{bmatrix}.$$

The characteristic equation of the Jacobian matrix J_{E_1} is given by

$$P_{J_{E_1}}(\lambda) = (c_2 v_1 - b_2 - \lambda)(c_1 y_1 - b_1 - \lambda)(\lambda^3 + \theta_1 \lambda^2 + \theta_2 \lambda + \theta_3),$$

where

$$\begin{aligned} \theta_1 &= \mu + \frac{r}{m} x_1 + \rho \frac{y_1}{x_1} + \frac{\eta_1 \delta_1 x_1}{\alpha_1 \mu} > 0, \\ \theta_2 &= \frac{\mu r x_1}{m} + \frac{\rho \mu y_1}{x_1} + \frac{\eta_1 \delta_1 \alpha v_1 x_1}{\alpha_1^2} + \frac{r \eta_1 \delta_1 x_1^2}{\alpha_1 \mu m} + \frac{r A v_1}{m} \eta \beta_2 y_1 > 0, \\ \theta_3 &= \frac{r \eta_1 \delta_1 \alpha v_1 x_1^2}{m \alpha_1^2} + \frac{\eta_1 \delta \mu v_1}{\alpha_1^2} + \frac{r A \mu v_1}{m} + \beta_2 \delta \mu y_1 > 0. \end{aligned}$$

Therefore, the eigenvalues are given by

$$\lambda_1 = c_2 v_1 - b_2, \quad \lambda_2 = c_1 y_1 - b_1 = \frac{c_1 \mu}{\delta_1} v_1 - b_1.$$

For $v_1 < \min \left\{ \frac{b_1 \delta_1}{c_1 \mu}, \frac{b_2}{c_2} \right\}$, we have $\lambda_1, \lambda_2 < 0$. The other eigenvalues of J_{E_1} have negative real parts. So the equilibrium point E_1 is locally asymptotically stable when $v_1 < \min \left\{ \frac{b_1 \delta_1}{c_1 \mu}, \frac{b_2}{c_2} \right\}$ and unstable when $v_1 > \frac{b_1 \delta_1}{c_1 \mu}$ or $v_1 > \frac{b_2}{c_2}$. □

Theorem 5.2. *The following holds:*

- (i) *If $\mathcal{R}_1 \leq 1$, then the equilibrium point E_2 does not exist.*
- (ii) *If $\mathcal{R}_1 > 1$ and $T_0 = \alpha_2(\delta + \rho)^2(1 - \mathcal{R}_1) + \frac{A \delta_1 \alpha_2 b_1}{c_1 \mu} \left(\frac{A \alpha \delta_1^2}{\mu^2} + A_2 \right) + \frac{\delta m b_1}{r c_1} A_2^2 < 0$, then the equilibrium point E_2 exists and it is locally asymptotically stable for $v_2 < \frac{b_2}{c_2}$.*

Proof. According to Descartes’s rule, there exists at least one positive real root $z = z_2$ for the equation

$$T_2 z^2 + T_1 z + T_0 = 0,$$

provided $T_2 > 0$ and $T_0 < 0$, with the coefficients defined in (5.2). We use the linearization method to study the local stability of the equilibrium point E_2 . The Jacobian matrix calculated at the equilibrium point E_2 is given by

$$J_{E_2} = \begin{bmatrix} -\frac{rx_2}{m} - \frac{\rho y_2}{x_2} & -\frac{rx_2}{m} + \rho - \beta_2 x_2 & -\frac{\eta_1 x_2}{\alpha_2^2} & 0 & 0 \\ \frac{\eta_1 v_2}{\alpha_2} + \beta_2 y_2 & -\frac{\eta_1 \delta_1 x_2}{\alpha_2 \mu} & \frac{\eta_1 x_2}{\alpha_2^2} & -\rho_1 y_2 & 0 \\ 0 & \delta_1 & -\mu & 0 & -\rho_2 v_2 \\ 0 & c_1 z_2 & 0 & 0 & 0 \\ 0 & 0 & 0 & 0 & c_2 v_2 - b_2 \end{bmatrix}.$$

The characteristic equation of the matrix J_{E_2} is given by

$$P_{J_{E_2}}(\lambda) = (c_2 v_2 - b_2 - \lambda)(\lambda^4 + n_1 \lambda^3 + n_2 \lambda^2 + n_3 \lambda + n_4),$$

where

$$\begin{aligned} n_1 &= \mu + \frac{r}{m} x_2 + \rho \frac{y_2}{x_2} + \frac{\eta_1 \delta_1 x_2}{\alpha_1 \mu}, \\ n_2 &= \rho_1 b_1 z_2 + \mu \left(\frac{r}{m} x_2 + \rho \frac{y_2}{x_2} \right) + \frac{\eta_1 \delta_1 \alpha v_2 x_2}{\alpha_2^2} + \frac{r \eta_1 \delta_1}{m \mu \alpha_2} x_2^2 + \frac{\beta_2 b_1}{c_1} (\delta + \rho_1 z_2) \\ &\quad + \frac{r b_1}{m c_1} (\delta + \rho + \rho_1 z_2), \\ n_3 &= \rho_1 b_1 z_2 \left(\frac{r}{m} x_2 + \rho \frac{y_2}{x_2} + \mu \right) + \frac{r \eta_1 \delta_1 \alpha v_2 x_2^2}{m \alpha_2^2} + \frac{r \mu^2 v_2}{m \delta_1} (\delta + \rho + \rho_1 z_2) \\ &\quad + \frac{\beta_2 \mu v_2}{\delta_1} (\delta + \rho_1 z_2), \\ n_4 &= \mu \delta_1 b_1 z_2 \left(\frac{r}{m} x_2 + \rho \frac{y_2}{x_2} \right) > 0. \end{aligned}$$

We have that $\lambda_1 = c_2 v_2 - b_2 < 0$ when $v_2 < \frac{b_2}{c_2}$. Now, we apply the Routh–Hurwitz criterion for the fourth-order polynomial $\lambda^4 + n_1 \lambda^3 + n_2 \lambda^2 + n_3 \lambda + n_4$ to study the remaining eigenvalues. On this basis, we compute

$$\Delta_1 = n_1 > 0, \quad \Delta_2 = n_1 n_2 - n_3 > 0, \quad \Delta_3 = \Delta_2 n_3 - (n_1 n_4) n_1 > 0.$$

That due to lengthy calculations, we will not write them here. Therefore, all the roots of the characteristic polynomial $\lambda^4 + n_1 \lambda^3 + n_2 \lambda^2 + n_3 \lambda + n_4$ have negative real parts, and hence, E_2 is locally asymptotically stable. □

Theorem 5.3. *The following statements are satisfied:*

- (i) *If $\mathcal{R}_0 \leq 1$, then the equilibrium point E_3 does not exist.*

(ii) If $\mathcal{R}_0 > 1$ and

$$Q_0 = rA^2\alpha_3^2 - mA\alpha_3(r-d)(B\alpha_3 + \eta_1) + rA\alpha_3A_1(B\alpha_3 + \eta_1) + m\delta A_3(B\alpha_3 + \eta_1)^2 < 0,$$

then the equilibrium point E_3 exists and it is locally asymptotically stable when $y_3 < \frac{b_1}{c_1}$.

Proof. If $\mathcal{R}_0 \leq 1$, then $Q_i > 0$ for $i = 0, 1, 2, 3$. Hence, we do not have any positive real root for w . We assume $\mathcal{R}_0 > 1$ and $Q_0 < 0$, then the equation

$$Q_3w^3 + Q_2w^2 + Q_1w + Q_0 = 0$$

has at least a positive real root and we get the equilibrium point $E_3 = (x_3, y_3, v_3, 0, w_3)$. The Jacobian matrix evaluated at E_3 is given by

$$J_{E_3} = \begin{bmatrix} -\frac{rx_3}{m} - \rho\frac{y_3}{x_3} & -\frac{rx_3}{m} + \rho - \beta_2x_3 & -\frac{\eta_1x_3}{\alpha_3^2} & 0 & 0 \\ \frac{\eta_1v_3}{\alpha_3} + \beta_2y_3 & -\frac{\eta_1v_3x_3}{\alpha_3y_3} & \frac{\eta_1x_3}{\alpha_3^2} & -\rho_1y_3 & 0 \\ 0 & \delta_1 & -\rho_2w_3 - \mu & 0 & -\rho_2v_3 \\ 0 & 0 & 0 & c_1y_3 - b_1 & 0 \\ 0 & 0 & c_2w_3 & 0 & 0 \end{bmatrix}.$$

The characteristic polynomial of the matrix J_{E_3} is as follows:

$$P_{J_{E_3}}(\lambda) = (c_1y_3 - b_1 - \lambda)(\lambda^4 + e_1\lambda^3 + e_2\lambda^2 + e_3\lambda + e_4),$$

where

$$e_1 = \rho_2w_3 + \frac{rx_3}{m} + \rho\frac{y_3}{x_3} + \frac{\eta_1v_3x_3}{\alpha_3y_3} + \mu > 0,$$

$$e_2 = \rho_2b_2w_3 + \mu(Nw_3 + 1)\left(\frac{rx_3}{m} + \rho\frac{y_3}{x_3}\right) + \frac{\eta_1\delta_1\alpha v_2x_3}{\alpha_3^2} + \frac{r}{m}x_3\left(\frac{rx_3}{m} + \rho\frac{y_3}{x_3} + \frac{\eta_1v_3}{\alpha_3} + \beta_2y_3\right) + \beta_2\delta y_3 > 0,$$

$$e_3 = \rho_2b_2w_3\left(\frac{rx_3}{m} + \rho\frac{y_3}{x_3} + \frac{\eta_1v_3x_3}{\alpha_3y_3}\right) + \frac{r\delta_1x_3y_3}{m\alpha_3}(\eta_1 + B(Nw_3 + 1)\alpha_3) + \frac{r\eta_1\delta_1x_3^2\alpha v_3}{m\alpha_3^2} + \frac{\eta_1\delta_1\delta y_3}{\alpha_3^2} > 0,$$

$$e_4 = \rho_2v_3w_3\left(\frac{r}{m}x_3\left(\frac{\eta_1v_3x_3}{\alpha_3y_3} + \frac{\eta_1v_3}{\alpha_3} + \beta_2y_3\right) + \beta_2\delta y_3\right) > 0.$$

One of the eigenvalues of the Jacobian matrix J_{E_3} is $\lambda_1 = c_1y_3 - b_2$, which is negative when $y_3 < \frac{b_1}{c_1}$. Now, to investigate the other eigenvalues of J_{E_3} , we apply the Routh–Hurwitz criterion to the fourth-order polynomial $\lambda^4 + e_1\lambda^3 + e_2\lambda^2 + e_3\lambda + e_4$, and we get

$$\Delta_1 = e_1 > 0, \quad \Delta_2 = e_1e_2 - e_3 > 0, \quad \Delta_3 = \Delta_2e_3 - (e_1e_4)e_1 > 0.$$

Thus, all the eigenvalues of the matrix J_{E_3} have negative real parts. Hence, the equilibrium point E_3 is locally asymptotically stable. \square

For the fourth endemic equilibrium point E_4 , we have the following result.

Theorem 5.4. *The following statements are satisfied:*

- (i) *If $\mathcal{R}_0 \leq 1$, then the equilibrium point E_4 does not exist.*
- (ii) *If $\mathcal{R}_0 > 1$ and*

$$\Psi_0 = rN_1^2 A^2 \alpha_4^2 - N_1 A \alpha_4 m (r - d) (BN_1 \alpha_4 + \eta_1) + ry_3 N_1 A \alpha_4 (BN_1 \alpha_4 + \eta_1) < 0,$$

then the endemic equilibrium point E_4 exists and it is locally asymptotically stable.

Proof. If $\mathcal{R}_0 \leq 1$, then $\Psi_i > 0$ for $i = 0, 1, 2$. Hence we do not have any positive value for z_4 . We assume $\mathcal{R}_0 > 1$ and $\Psi_0 < 0$. Then, the equation $\Psi_2 z^2 + \Psi_1 z + \Psi_0 = 0$, with the coefficients defined in (5.3), has exactly one positive root $z = z_4 = \frac{-\Psi_1 + \sqrt{\Delta}}{2\Psi_2}$, where $\Delta = \Psi_1^2 - 4\Psi_0\Psi_2$. So we get the unique equilibrium point $E_4 = (x_4, y_4, v_4, z_4, w_4)$. To analyze its stability, we compute the Jacobian matrix at the point E_4 , which is given by

$$J_{E_4} = \begin{bmatrix} -\frac{rx_4}{m} - \rho \frac{y_4}{x_4} & -\frac{rx_4}{m} + \rho - \beta_2 x_4 & -\frac{\eta_1 x_4}{\alpha_4^2} & 0 & 0 \\ \frac{\eta_1 v_4}{\alpha_4} + \beta_2 y_4 & -\frac{\eta_1 v_4 x_4}{\alpha_4 y_4} & \frac{\eta_1 x_4}{\alpha_4^2} & -\rho_1 y_4 & 0 \\ 0 & \delta_1 & -\rho_2 w_4 - \mu & 0 & -\rho_2 v_4 \\ 0 & c_1 z_4 & 0 & 0 & 0 \\ 0 & 0 & c_2 w_4 & 0 & 0 \end{bmatrix}.$$

The characteristic polynomial of the matrix J_{E_4} is obtained as follows:

$$P_{J_{E_4}}(\lambda) = \lambda^5 + q_1 \lambda^4 + q_2 \lambda^3 + q_3 \lambda^2 + q_4 \lambda + q_5,$$

where

$$\begin{aligned} q_1 &= \rho_1 w_4 + \frac{r}{m} x_4 + \rho \frac{y_4}{x_4} + \frac{\eta_1 \delta_1 x_4}{\alpha_4 \mu} + \mu > 0, \\ q_2 &= c_1 \rho_1 y_4 z_4 + c_2 \rho_2 v_4 w_4 + \mu N_1 \left(\frac{r}{m} x_4 + \rho \frac{y_4}{x_4} \right) + \frac{\eta_1 \delta_1 \alpha v_4 x_4}{\alpha_4^2} + \frac{r \eta_1 v_4 x_4^2}{m \alpha_4 y_4} \\ &\quad + \delta \beta_2 y_4 + \beta_2 v_4 N_2 z_4 + \frac{r x_4 v_4}{m \alpha_4} (\eta_1 + BN_1 \alpha_4) > 0, \\ q_3 &= (\rho_2 b_2 w_4 + \rho_1 b_1 z_4) \left(\frac{r}{m} x_4 + \rho \frac{y_4}{x_4} + \frac{\eta_1 \delta_1 x_4}{\alpha_4 \mu} \right) + b_1 \rho_1 \rho_2 w_4 z_4 + b_1 \mu \rho_1 z_4 \\ &\quad + \frac{r \eta_1 \delta_1 \alpha v_4 x_4^2}{m \alpha_4^2} + \mu N_1 \delta \beta_2 y_4 + \mu N_1 \beta_2 v_4 N_2 z_4 + \frac{r \mu N_1 x_4 v_4}{m \alpha_4} (\eta_1 + BN_1 \alpha_4) \end{aligned}$$

$$\begin{aligned}
 & + \frac{\eta_1 \delta_1 v_4}{\alpha_4^2} (\delta y_4 + N_2 z_4) > 0, \\
 q_4 & = \rho_1 \rho_2 b_1 b_2 z_4 w_4 + \rho_1 b_1 z_4 \mu N_1 \left(\frac{r}{m} x_4 + \rho \frac{y_4}{x_4} \right) \\
 & + \rho_2 b_2 w_4 \left(\frac{r \eta_1 v_4 x_4^2}{m \alpha_4 y_4} + \delta \beta_2 y_4 + \beta_2 v_4 N_2 z_4 + \frac{r x_4 v_4}{m \alpha_4} (\eta_1 + B N_1 \alpha_4) \right) > 0, \\
 q_5 & = \rho_1 \rho_2 b_1 b_2 w_4 z_4 \left(\frac{r}{m} x_4 + \rho \frac{y_4}{x_4} \right) > 0.
 \end{aligned}$$

By using the Routh–Hurwitz criterion for the fifth-order polynomials, we get

$$\begin{aligned}
 \Delta_1 & = q_1 > 0, & \Delta_2 & = q_1 q_2 - q_3 > 0, \\
 \Delta_3 & = \Delta_2 q_3 - q_1^2 q_4 > 0, & \Delta_4 & = \Delta_3 q_4 - \Delta_2 q_2 q_5 + q_1 q_4 q_5 - q_5^2 > 0.
 \end{aligned}$$

As $\Delta_3 q_4 + q_1 q_4 q_5 > \Delta_2 q_2 q_5 + q_5^2$, we deduce that $\Delta_4 > 0$. This implies that all the eigenvalues of the Jacobian matrix J_{E_4} have negative real parts. Therefore E_4 is locally asymptotically stable. □

6. Analysis of the basic reproductive number

In this section, we analyze the basic production rate, and we examine the effect of different parameters for the viral load related to the basic reproduction number, \mathcal{R}_1 , mentioned in the equation (4.1). The basic production number indicates the prevalence of infection in the population, and it is important ideas in epidemic theory for mathematicians [17]. The different ways exist for behavior Sensitivity Analysis. In this section, we apply the normalized forward index. The normalized forward index is defined as follows:

$$\Theta_s^{\mathcal{R}_1} = \left(\frac{\partial \mathcal{R}_1}{\partial s} \right) \left(\frac{s}{\mathcal{R}_1} \right),$$

where s states existence parameters in (4.1). By replacing $\eta_1 = (1 - \eta)\beta_1$, $A = \frac{\mu(\delta + \rho)}{\delta_1}$, $B = \frac{\beta_2 \mu}{\delta_1}$, and $\delta_1 = (1 - \varepsilon)n\delta$ in \mathcal{R}_1 , we obtain

$$(6.1) \quad \mathcal{R}_1 = \frac{m(r - d)\{(1 - \eta)(1 - \varepsilon)n\delta\beta_1 + \beta_2\mu\}}{\mu(\delta + \rho)},$$

that with partial derivation (6.1) respect to s , we get

$$\begin{aligned}
 \frac{\partial \mathcal{R}_1}{\partial m} \frac{m}{\mathcal{R}_1} & = 1, \\
 \frac{\partial \mathcal{R}_1}{\partial r} \frac{r}{\mathcal{R}_1} & = \frac{d}{r - d}, \\
 \frac{\partial \mathcal{R}_1}{\partial d} \frac{d}{\mathcal{R}_1} & = -\frac{d}{r - d},
 \end{aligned}$$

$$\begin{aligned}
 (6.2) \quad \frac{\partial \mathcal{R}_1}{\partial n} \frac{n}{\mathcal{R}_1} &= \frac{(1-\eta)(1-\varepsilon)n\delta\beta_1}{(1-\eta)(1-\varepsilon)n\delta\beta_1 + \beta_2\mu}, \\
 \frac{\partial \mathcal{R}_1}{\partial \delta} \frac{\delta}{\mathcal{R}_1} &= \frac{\delta}{\delta + \rho} \left[\frac{(1-\eta)(1-\varepsilon)n\rho\beta_1 - \beta_2\mu}{(1-\eta)(1-\varepsilon)n\delta\beta_1 + \beta_2\mu} \right], \\
 \frac{\partial \mathcal{R}_1}{\partial \beta_1} \frac{\beta_1}{\mathcal{R}_1} &= \frac{(1-\eta)(1-\varepsilon)n\delta\beta_1}{(1-\eta)(1-\varepsilon)n\delta\beta_1 + \beta_2\mu}, \\
 \frac{\partial \mathcal{R}_1}{\partial \beta_2} \frac{\beta_2}{\mathcal{R}_1} &= \frac{\beta_2\mu}{(1-\eta)(1-\varepsilon)n\delta\beta_1 + \beta_2\mu}, \\
 \frac{\partial \mathcal{R}_1}{\partial \mu} \frac{\mu}{\mathcal{R}_1} &= -\frac{(1-\eta)(1-\varepsilon)n\delta\beta_1}{(1-\eta)(1-\varepsilon)n\delta\beta_1 + \beta_2\mu}, \\
 \frac{\partial \mathcal{R}_1}{\partial \rho} \frac{\rho}{\mathcal{R}_1} &= -\frac{\rho}{\delta + \rho}, \\
 \frac{\partial \mathcal{R}_1}{\partial \eta} \frac{\eta}{\mathcal{R}_1} &= -\frac{(1-\varepsilon)n\delta\beta_1\eta}{(1-\eta)(1-\varepsilon)n\delta\beta_1 + \beta_2\mu}, \\
 \frac{\partial \mathcal{R}_1}{\partial \varepsilon} \frac{\varepsilon}{\mathcal{R}_1} &= -\frac{(1-\eta)n\delta\beta_1\varepsilon}{(1-\eta)(1-\varepsilon)n\delta\beta_1 + \beta_2\mu}.
 \end{aligned}$$

The index (6.2) obtained from the parameters existing in the system (2.1) indicates the sensitivity of the system parameters. It is positive for the parameters r, m, n, β_1 and β_2 , which means that increasing them raises the reproduction rate number \mathcal{R}_1 and as a result the disease spreads. While this index is negative for the parameters $d, \rho, \eta, \varepsilon$ and μ and it shows that increasing these parameters decreases the reproduction rate number \mathcal{R}_1 . When the value of \mathcal{R}_1 reaches less than one, the disease disappear. When $(1-\eta)(1-\varepsilon)n\rho\beta_1 - \beta_2\mu > 0$, the index for δ is positive and the index is negative for $(1-\eta)(1-\varepsilon)n\rho\beta_1 - \beta_2\mu < 0$.

7. Numerical simulation

7.1. Stability of equilibrium points

In this section, we examine the theoretical results of model (2.1) by numerical simulations. First, we illustrate the stability of equilibrium points for the different values of \mathcal{R}_0 and \mathcal{R}_1 . In the following, we examine the effect of cell-to-cell transmission on the spread of infection for different values β_2 . Then, the sensitivity analysis is used to identify important factors in increasing or decreasing the rate of reproduction. The parameters of ρ_2, c_2 and b_2 may vary with different types of antibodies [35]. Initial values in Table 7.2 are expressed according to clinical data of HIV-infected patients during the symptomatic phase [16]. Since several biological studies indicate that some patients with HIV are treated after three to six months, our chosen interval will change between 100 days to 150 days [24]. In Figure 7.1, by using from Column 1 of Table 7.1, we have $\mathcal{R}_0 = 0.41 < 1$, then

$E_0 = (0, 0, 0, 0, 0)$ or disease-free equilibrium point is stable. It shows that the treatment reduces the virus load and the disease will disappear.

Parameters	unit	Column 1	Column 2	Column 3	Column 4	Column 5	Column 6	References
r	day^{-1}	0.0082	2	2	2	2	2	Assumed
m		1000	1000	15000	100000	5×10^4	300000	Assumed
β_1	$ml \cdot (virion \cdot day)^{-1}$	4.8×10^{-7}	[34]					
β_2	$ml \cdot (virion \cdot day)^{-1}$	4.7×10^{-7}	[34]					
α	$cells^{-1} \cdot ml$	0.001	0.001	0.001	0.001	0.001	0.001	[8, 12, 32, 33]
ρ	day^{-1}	0.01	0.01	0.01	0.01	0.01	0.01	[8, 12, 32, 33]
d	day^{-1}	0.02	0.02	0.02	0.02	0.02	0.02	[8, 12, 32, 33]
δ	day^{-1}	0.5	0.5	0.5	0.5	0.5	0.5	[8, 12, 32, 33]
ρ_1	$ml \cdot (cells \cdot day)^{-1}$	0.001	0.001	0.001	0.001	0.001	0.001	[8, 12, 32, 33]
η		0.4	0.4	0.1	0.55	0.55	0.55	[8, 12, 32, 33]
ε		0.55	0.55	0.2	0.45	0.45	0.2	[8, 12, 32, 33]
n	$ml \cdot virion$	1200	1200	1200	1200	1200	1200	[8, 12, 32, 33]
μ	day^{-1}	3	3	3	3	3	3	[8, 12, 32, 33]
ρ_2	$ml \cdot (virion \cdot day)^{-1}$	0.5	0.5	0.5	0.001	0.001	0.001	[35]
c_1	$ml \cdot (cells \cdot day)^{-1}$	0.021	0.021	0.021	0.021	0.021	0.021	Assumed
b_1	day^{-1}	0.2	0.2	0.2	0.2	0.2	0.2	[8, 12, 32, 33]
c_2	$ml \cdot (virion \cdot day)^{-1}$	10^{-11}	10^{-11}	10^{-11}	10^{-11}	10^{-4}	10^{-4}	[35]
b_2	day^{-1}	0.1	0.1	0.1	0.1	0.01	0.1	[35]

Table 7.1: Values of parameters in HIV mathematical model.

Variables	Initial value	unit
$x(t)$	$x(0) = 200$	$cell \cdot ml^{-1}$
$y(t)$	$y(0) = 80$	$cell \cdot ml^{-1}$
$v(t)$	$v(0) = 12000$	$cell \cdot ml^{-1}$
$z(t)$	$z(0) = 50$	$cell \cdot ml^{-1}$
$w(t)$	$w(0) = 100$	$cell \cdot ml^{-1}$

Table 7.2: The initial values in HIV mathematical model.

s	value
m	1
r	0.01010101057
d	-0.01010101010
n	0.9932461561
δ	0.01285399907
β_1	0.9932461561
β_2	0.006753843943
μ	-0.9932461565
ρ	-0.01960784314
η	-0.1103606840
ε	-0.2483115390

Table 7.3: The calculated values of $\Theta_s^{\mathcal{R}1}$.

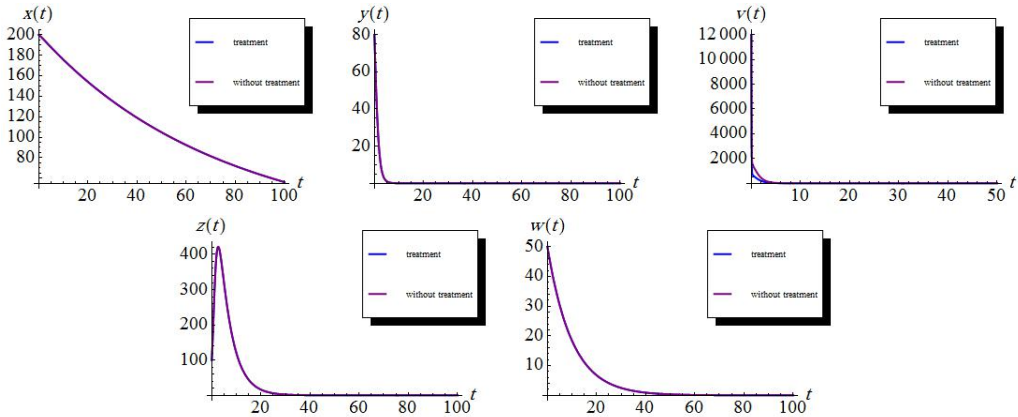


Figure 7.1: The integral curves of the solutions $x(t)$, $y(t)$, $v(t)$, $z(t)$ and $w(t)$ of system (2.1) with treatment and without treatment for Column 1 of Table 7.1 at time t for $\mathcal{R}_0 = 0.41 < 1$ at free-equilibrium point of $E_0 = (0, 0, 0, 0, 0)$.

In Figure 7.2, from Column 2 of Table 7.1, we obtain $\mathcal{R}_1 = 0.05122764706 < 1$ and $\mathcal{R}_0 = 100 > 1$, then $E_{01} = (990, 0, 0, 0, 0)$ is asymptotically stable. This leads to the saturation of the population of uninfected cells and eventually eliminate the disease.

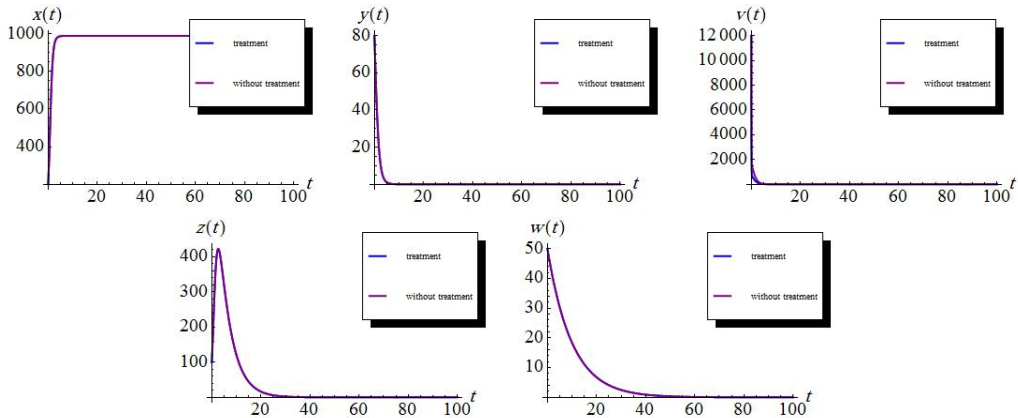


Figure 7.2: The integral curves of the solutions $x(t)$, $y(t)$, $v(t)$, $z(t)$ and $w(t)$ of system (2.1) with treatment and without treatment at time t for Column 2 of Table 7.1 with $\mathcal{R}_0 = 100 > 1$ and $\mathcal{R}_1 = 0.05122764706 < 1$ at $E_{01} = (990, 0, 0, 0, 0)$.

In Figure 7.3, by replacing values from Column 3 of Table 7.1 in system (2.1), we obtain $\mathcal{R}_1 = 2.026297059 > 1$ that despite the condition $\psi_0 = -0.0002085467695 < 0$, we have $E_1 = (14841.86236, 6.496271350, 1039.403416, 0, 0)$ is asymptotically stable. In other words, by increasing the proliferation rate of the uninfected cells population and decreasing the level of treatment relative to Column 2, the values of infected cells and the

virus in Table 7.1 are decreased such that they converge to y_1 and v_1 . Still, the levels of cellular and humoral immune cells converge to zero.

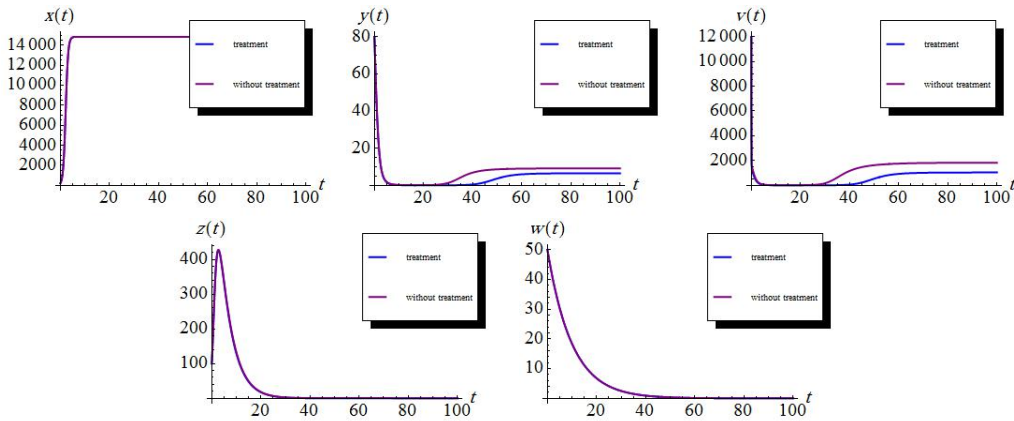


Figure 7.3: The integral curves of the solutions $x(t)$, $y(t)$, $v(t)$, $z(t)$ and $w(t)$ of system (2.1) with treatment and without treatment at time t for Column 3 of Table 7.1 with $\mathcal{R}_1 = 2.026297059 > 1$ and $\psi_0 = -0.0002085467695 < 0$ at $E_1 = (14841.86236, 6.496271350, 1039.403416, 0, 0)$.

In Figure 7.4, from Column 4 of Table 7.1, we obtain $\mathcal{R}_1 = 4.703470589 > 1$ and since $T_0 = -1.464981642 < 0$, the equilibrium $E_2 = (98984.77489, 9.523809524, 1047.619048, 685.1145481, 0)$ exists and it is asymptotically stable. This means that treatment reduces the level of proliferation of viral and infectious cells and prevents excessive cellular immunity.

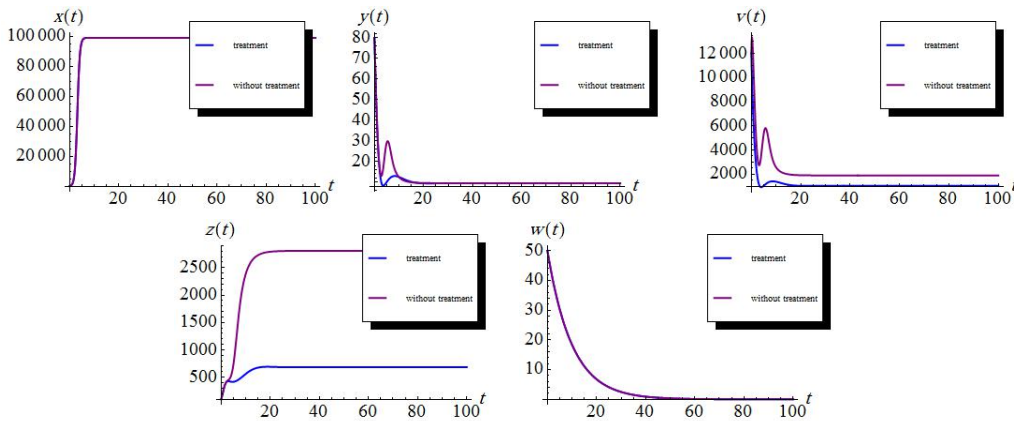


Figure 7.4: The integral curves of the solutions $x(t)$, $y(t)$, $v(t)$, $z(t)$ and $w(t)$ of system (2.1) with treatment and without treatment at time t for Column 4 of Table 7.1 with $\mathcal{R}_1 = 4.703470589 > 1$ and $T_0 = -1.464981642 < 0$ at $E_2 = (98984.77489, 9.523809524, 1047.619048, 685.1145481, 0)$.

In Figure 7.5, we choose parameters from Column 5 of Table 7.1 into system (2.1) and derive $\mathcal{R}_1 = 2.351735294 > 1$ and $Q_0 = -0.00005940827650 < 0$. Then, it can be concluded that $E_3 = (49497.49885, 1.996874149, 100, 0, 3589.684691)$ is an equilibrium point and it is asymptotically stable. By observing Figure 7.5, stimulation of the humoral immune system and timely treatment can significantly reduce virus replication and the number of infected cells.

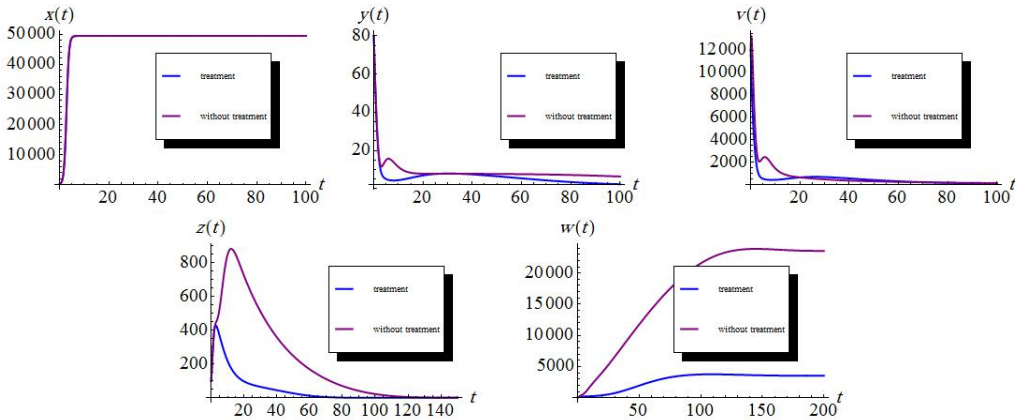


Figure 7.5: The integral curves of the solutions $x(t)$, $y(t)$, $v(t)$, $z(t)$ and $w(t)$ of system (2.1) with treatment and without treatment at time t for Column 5 of Table 7.1 with $\mathcal{R}_1 = 2.351735294 > 1$ and $Q_0 = -0.00005940827650 < 0$ at $E_3 = (49497.49885, 1.996874149, 100, 0, 3589.684692)$.

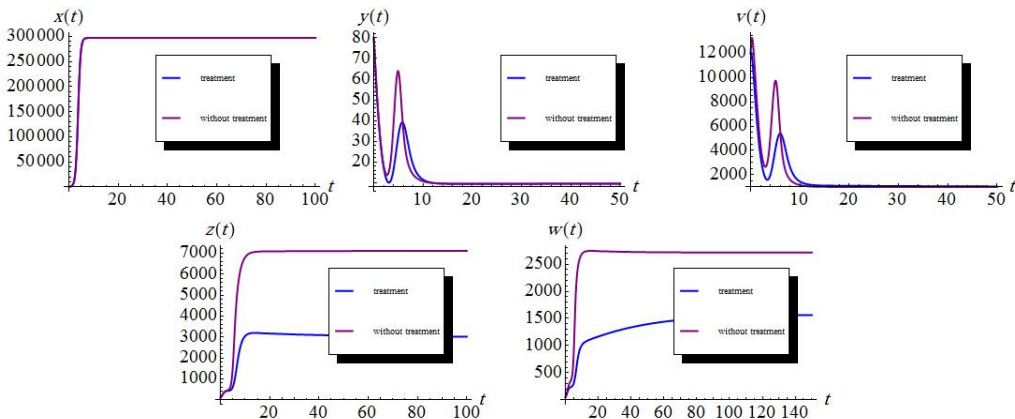


Figure 7.6: The integral curves of the solutions $x(t)$, $y(t)$, $v(t)$, $z(t)$ and $w(t)$ of system (2.1) with treatment and without treatment at time t for Column 6 of Table 7.1 with $\mathcal{R}_1 = 20.39982353 > 1$ and $\Psi_0 = -0.001109190902 < 0$ at $E_4 = (296974, 9.523809524, 1000, 2997.258841, 1571.428572)$.

We find $\mathcal{R}_1 = 20.39982353 > 1$ and $\Psi_0 = -0.001109190902 < 0$ for parameters chosen from Column 6 of Table 7.1; see Figure 7.6. Therefore, $E_4 = (296974, 9.523809524, 1000, 2997.258841, 1571.428572)$ is the asymptotically stable equilibrium point for the differential system. In this case, trajectories associated with different initial values typically converge to this equilibrium. Here, the virus load is controlled by the treatment, yet the virus remains in the body.

We simulate the stability of E_4 by the Routh Hurwitz method. The Jacobian matrix at the point E_4 is given by

$$J_{E_4} = \begin{bmatrix} -1.979824674 & -2.109401970 & -0.01603657726 & 0 & 0 \\ 0.0001124761905 & -3.367681224 & 0.01603657726 & -0.009523809524 & 0 \\ 0 & 480.0 & -4.571428572 & 0 & -1.0 \\ 0 & 62.94243566 & 0 & 0.0 & 0 \\ 0 & 0 & 0.1571428572 & 0 & 0.0 \end{bmatrix}.$$

The characteristic polynomial of matrix J_{E_4} is obtained as follows:

$$P_{J_{E_4}}(\lambda) = \lambda^5 + 9.918934470\lambda^4 + 24.17243443\lambda^3 + 20.00924654\lambda^2 + 6.567388432\lambda + 0.186498605.$$

The Routh Hurwitz table is derived as

$$RR = \begin{bmatrix} 1 & \frac{2417243443}{100000000} & \frac{410461777}{62500000} & \lambda^5 \\ \frac{991893447}{100000000} & \frac{1000462327}{50000000} & \frac{37299721}{200000000} & \lambda^4 \\ \frac{2197555465515418021}{99189344700000000} & \frac{405968730569025319}{61993340437500000} & 0 & \lambda^3 \\ \frac{9382146379552317657964235963}{549388866378854505250000000} & \frac{37299721}{200000000} & 0 & \lambda^2 \\ \frac{118339541585510199203652409882048623457}{18764292759104635315928471926000000000} & 0 & 0 & \lambda \\ \frac{37299721}{200000000} & 0 & 0 & 1 \end{bmatrix}.$$

There is no change of sign in the first Column of the Routh Hurwitz table. Hence, $P_{J_{E_4}}(\lambda)$ has no positive root. We derive the Routh Hurwitz table for computing the number of negative roots as

$$RL = \begin{bmatrix} 1 & \frac{2417243443}{100000000} & \frac{410461777}{62500000} & \lambda^5 \\ -\frac{991893447}{100000000} & -\frac{1000462327}{50000000} & -\frac{37299721}{200000000} & \lambda^4 \\ \frac{2197555465515418021}{99189344700000000} & \frac{405968730569025319}{61993340437500000} & 0 & \lambda^3 \\ -\frac{9382146379552317657964235963}{549388866378854505250000000} & -\frac{37299721}{200000000} & 0 & \lambda^2 \\ \frac{118339541585510199203652409882048623457}{18764292759104635315928471926000000000} & 0 & 0 & \lambda \\ -\frac{37299721}{200000000} & 0 & 0 & 1 \end{bmatrix}.$$

There are five sign changes in the first Column of table RL. Thereby, $P_{J_{E_4}}(\lambda)$ has five negative roots.

Figure 7.7 depicts the impact of the accident rate β_2 on the infection cell-to-cell transmissions (i.e., through cell-to-cell transmission) for different values of $\beta_2 = 0, 0.00000047,$ and 0.0000047 .

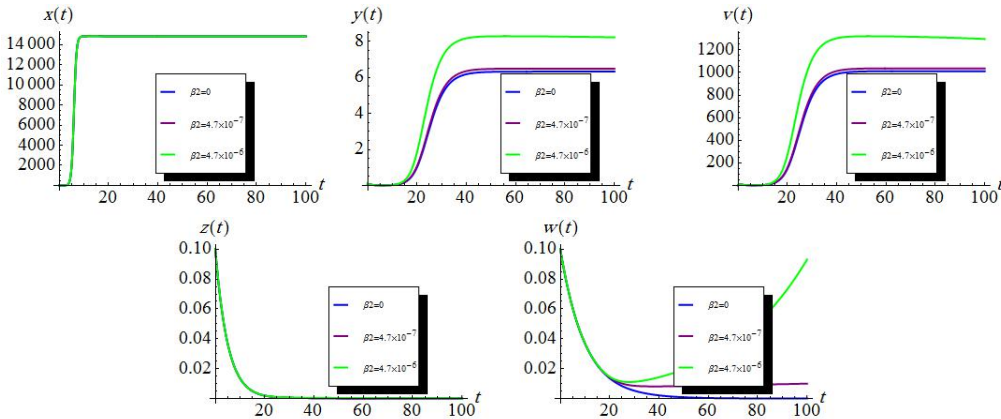


Figure 7.7: The integral curves of the solutions $x(t), y(t), v(t), z(t)$ and $w(t)$ of system (2.1) for different values of β_2 .

By using values from Column 3 of Table 7.1, we compute the reproduction rate numbers in Table 7.3. These illustrate the role of essential parameters in the system for the increase or decrease of the infection.

7.2. Global dynamics and convergence dynamics

For reproduction rate number $\mathcal{R}_1 > 1$, model (2.1) has four equilibrium points, where only E_4 is an internal (positive) equilibrium point (see Theorem 5.4). Numerical simulation shows that model (2.1) with parameter values taken from Column 3 of Table 7.1 has only one equilibrium point $E_1 = (14841.86236, 6.496271350, 1039.403416, 0, 0)$. Solutions starting from any initial point with non-negative coordinates converge to E_1 . See Figure 7.8. Model (2.1) with parameter values given in Column 4 of Table 7.1 has two equilibrium points $E_2 = (98984.77489, 9.523809524, 1047.619048, 685.1145481, 0)$ and $E_1 = (98953.6, 37.0242, 4073, 0, 0)$. The linear subspace $\{z = w = 0\}$ is an invariant manifold and thus, in this case, the solutions starting from this subspace converge to E_1 . However, the solutions starting from outside this subspace converge to E_2 . See Figure 7.9. When the cellular immune and humoral immune cells are not active in the body, these immune factors may remain inactive. However, any small activity in either the cellular immune or humoral immune leads to an amplification of the cellular immune (up to 685.1145481) while the humoral immune collapses to zero.

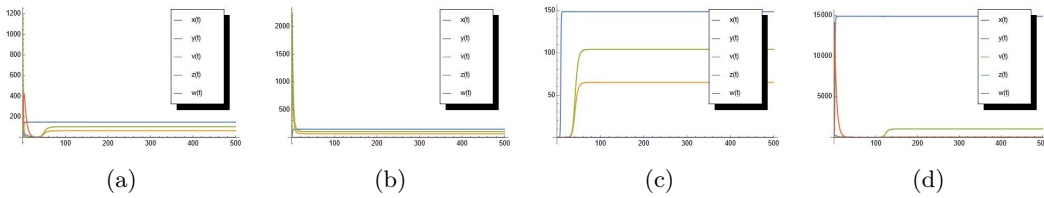


Figure 7.8: The integral curves of system (2.1) in the rescaled space with the parameter values given in Column 3 of Table 7.1 and with different initial values. (a) $x(0) = 200$, $y(0) = 80$, $v(0) = 12000$, $z(0) = 100$, $w(0) = 50$, (b) $x(0) = 1000$, $y(0) = 200$, $v(0) = 500$, $z(0) = 0$, $w(0) = 0$, (c) $x(0) = 0.001$, $y(0) = 0.001$, $v(0) = 0.001$, $z(0) = 0.001$, $w(0) = 0.001$ and (d) $x(0) = 2000$, $y(0) = 800$, $v(0) = 13000$, $z(0) = 300$, $w(0) = 500$ converging to $E_1 = (14841.86236, 6.496271350, 1039.403416, 0, 0)$.

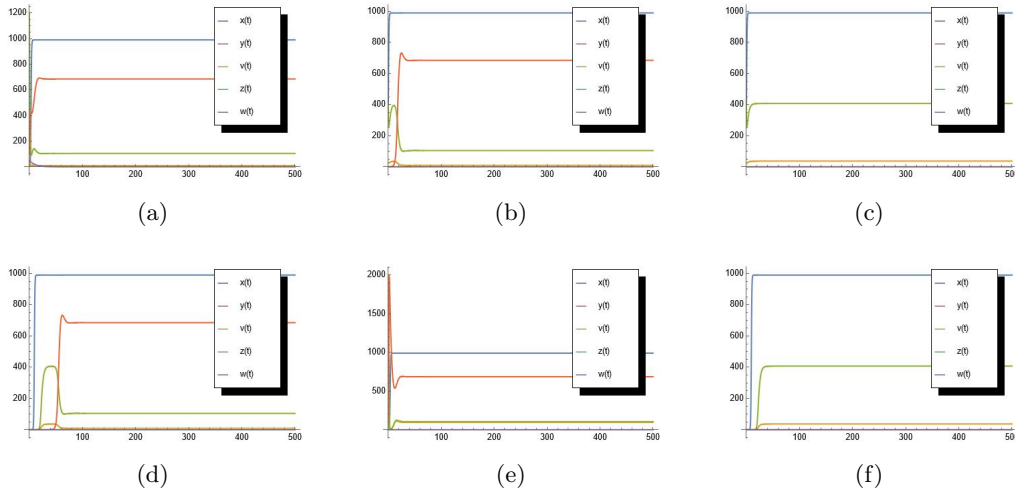


Figure 7.9: The integral curves of system (2.1) in the rescaled space with the parameter values given in Column 4 of Table 7.1 and with different initial values. (a) $x(0) = 200$, $y(0) = 80$, $v(0) = 12000$, $z(0) = 100$, $w(0) = 50$, (b) $x(0) = 36000$, $y(0) = 25$, $v(0) = 4037$, $z(0) = 0.1$, $w(0) = 0.1$, (c) $x(0) = 36000$, $y(0) = 25$, $v(0) = 4037$, $z(0) = 0$, $w(0) = 0$, (d) $x(0) = 0.001$, $y(0) = 0.001$, $v(0) = 0.001$, $z(0) = 0.001$, $w(0) = 0.001$, (e) $x(0) = 100$, $y(0) = 200$, $v(0) = 100$, $z(0) = 100$, $w(0) = 0$, (f) $x(0) = 0.001$, $y(0) = 0.001$, $v(0) = 0.001$, $z(0) = 0$, $w(0) = 0$ converging to $E_1 = (98953.6, 37.0242, 4072.66, 0, 0)$ and $E_2 = (98984.77489, 9.523809524, 1047.619048, 685.1145481, 0)$.

If we use the parameter values given in Column 5 of Table 7.1, then model (2.1) admits three equilibrium points $E_3 = (49497.49885, 1.996874149, 100, 0, 3589.684692)$, $E_2 = (49487.6, 9.5, 1048, 87.5001, 0)$ and $E_1 = (17534.8, 8.847, 1415.5, 0, 0)$. In this case, all so-

lutions starting from outside the invariant subspace $\{w = 0\}$ converge to E_3 ; the solutions with initial values $z = w = 0$ converge to E_1 , and the other solutions with $w = 0$ converge to E_2 . See Figure 7.10. Here, we have three equilibria. When immune of cellular is inactive and humoral immune is active, the cellular dynamics of the system converge to E_3 . Since the cellular immune of E_3 is zero, the cellular immune in the body remains inactive. By simulating the model with the parameter values from Column 6 of Table 7.1, we see that there are four equilibrium points $E_1 = (171905, 166.8, 26683.9, 0, 0)$, $E_2 = (296970, 9.5, 1524, 3696.2, 0)$, $E_3 = (296892, 86.55, 1000, 0, 38545)$, and $E_4 = (296974, 9.523809524, 1000, 2997.258841, 1571.428572)$. By choosing different initial values, we observe that the solutions with any initial point with positive coordinates converge to E_4 . But the solutions with $z = w = 0$ converge to E_1 , the solutions with $w = 0$ and $z \neq 0$ converge to E_2 , and the solutions with $z = 0$ and $w \neq 0$ converge to E_3 . See Figure 7.11. The above simulation suggests that E_4 is globally asymptotically stable. Among the equilibria, E_4 stands to attract the cellular dynamics of the system for when immune of cellular and humoral are both active.

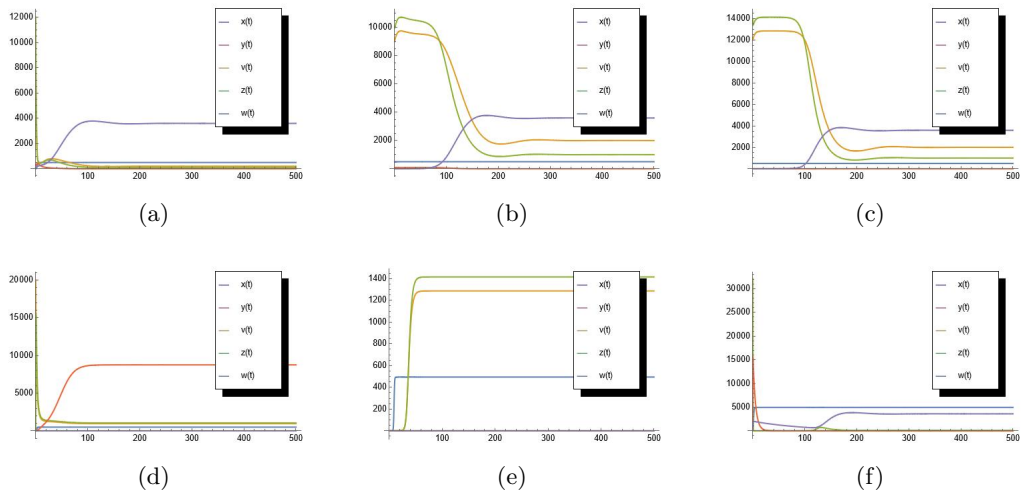


Figure 7.10: The integral curves of system (2.1) in the rescaled space with the parameter values given in Column 5 of Table 7.1 and with different initial values. (a) $x(0) = 200$, $y(0) = 80$, $v(0) = 12000$, $z(0) = 100$, $w(0) = 50$, (b) $x(0) = 49000$, $y(0) = 9$, $v(0) = 1000$, $z(0) = 80$, $w(0) = 0.1$, (c) $x(0) = 49000$, $y(0) = 12$, $v(0) = 1400$, $z(0) = 0.001$, $w(0) = 0.001$, (d) $x(0) = 1000$, $y(0) = 200$, $v(0) = 0.001$, $z(0) = 0.001$, $w(0) = 0$, (e) $x(0) = 0.001$, $y(0) = 0.001$, $v(0) = 0.001$, $z(0) = 0$, $w(0) = 0$, (f) $x(0) = 2000$, $y(0) = 800$, $v(0) = 13000$, $z(0) = 1000$, $w(0) = 500$ converging to $E_1 = (49483.9, 12.8684, 1415.52, 0, 0)$, $E_2 = (49487.6, 9.52381, 1047.62, 87.5001, 0)$ and $E_3 = (49497.49885, 1.996874149, 100, 0, 3589.684692)$.

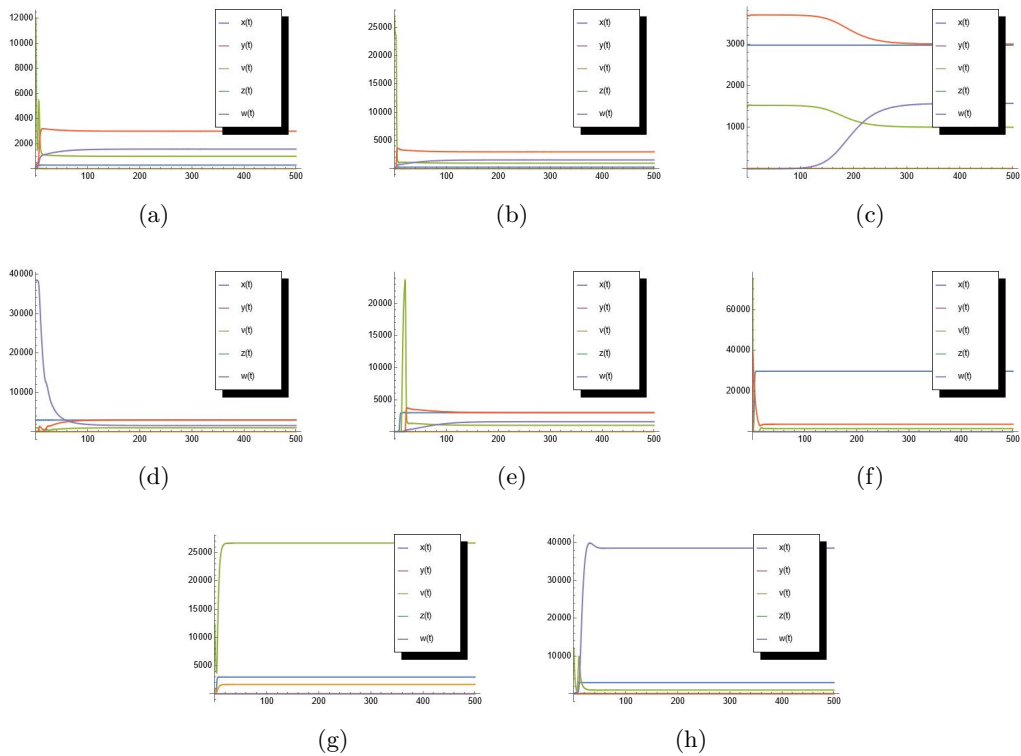


Figure 7.11: The integral curves of system (2.1) in the rescaled space with the parameter values given in Column 5 of Table 7.1 and with different initial values. (a) $x(0) = 200$, $y(0) = 80$, $v(0) = 12000$, $z(0) = 100$, $w(0) = 50$, (b) $x(0) = 296000$, $y(0) = 166$, $v(0) = 26600$, $z(0) = 0.1$, $w(0) = 0.1$, (c) $x(0) = 296900$, $y(0) = 9$, $v(0) = 1500$, $z(0) = 3690$, $w(0) = 0.1$, (d) $x(0) = 296800$, $y(0) = 86$, $v(0) = 999$, $z(0) = 0.1$, $w(0) = 38500$, (e) $x(0) = 0.001$, $y(0) = 0.001$, $v(0) = 0.001$, $z(0) = 0.001$, $w(0) = 0.001$, (f) $x(0) = 1000$, $y(0) = 2000$, $v(0) = 1000$, $z(0) = 500$, $w(0) = 0$, (g) $x(0) = 200$, $y(0) = 80$, $v(0) = 12000$, $z(0) = 0$, $w(0) = 0$, (h) $x(0) = 0$, $y(0) = 80$, $v(0) = 12000$, $z(0) = 0$, $w(0) = 50$ converging to $E_1 = (296791, 166.774, 26683.9, 0, 0)$, $E_2 = (296970, 9.52381, 1523.81, 3696.16, 0)$, $E_3 = (296892, 86.5524, 1000, 0, 38545.2)$ and $E_4 = (296974, 9.523809524, 1000, 2997.258841, 1571.428572)$.

8. Conclusion

In this paper, we first formulate and then analyse a definitive in-vivo mathematical model for the dynamics of the human immunodeficiency virus (HIV). This model investigates the effect of cellular and humoral immune response on the CD_4^+ uninfected cells, the CD_4^+ infected cells, and the virus. Since infected CD_4^+ T-cells affect the rate of proliferation of uninfected CD_4^+ T-cells, the rate of the spread of uninfected CD_4^+ T-cells in the model

was considered as a logistic function. Also, in this model, the effect of cell-to-cell and virus-to-cell transmission in the spread of the disease have considered. In this model, the rate of cure and its impact on improving infected CD_4^+ T-cells to uninfected CD_4^+ T-cells have impacted. Then, compatibility with biological hypotheses, the boundedness, and the non-negativity of solutions was proved. We also showed that this model has six equilibrium points, including two free infection points and four endemic points. Then, the equilibrium points asymptotic stability was investigated by the Routh Hurwitz method. The treatment parameters were considered as two parameters (the effectiveness of Reverse Transcriptase and Protease Inhibitors) time-independent in the model (2.1) and were examined their dynamics. Since global dynamic is biologically relevant, global dynamic analysis for various parameter values and the infected equilibrium points of model (2.1) is numerically examined. In all cases, the treatment is not sufficient to eliminate the disease and the virus remains in the body once the body is infected. However, the treatment appears to beneficial to control the amount of virus in the body and rate of infections.

Entry of any amount of virus into the body and the production of infected cells cause initial increases in cellular and humoral immune cells. However, they are finally stabilized and the treatment balances the number of viruses, healthy and infected cells. In there words, the virus load, the number of infected and healthy cells, cellular and humoral immune systems are either reduced or increased according to their relative values to the globally asymptotic equilibrium point E_4 .

Finally, by simulating the model (2.1), using Mathematica and Mapple software, the convergence of equilibrium points for the appropriate parameters, the effect of the cell-to-cell transfer on disease spread, sensitivity analysis of reproduction for some parameters, and its effect on decreasing or increasing this amount was shown.

References

- [1] A. K. Abbas, A. H. Lichtman and S. Pillai, *Cellular and Molecular Immunology E-Book*, Elsevier Health Sciences, 2014.
- [2] N. Ali, G. Zaman, Abdullah, A. M. Alqahtani and A. S. Alshomrani, *The effects of time lag and cure rate on the global dynamics of HIV-1 model*, BioMed Res. Int. **2017**, Art. ID 8094947, 11 pp.
- [3] J. B. Alimonti, T. B. Ball and K. R. Fowke, *Mechanisms of CD_4^+ T lymphocyte cell death in human immunodeficiency virus infection and AIDS*, J. Gen. Virol. **84** (2003), no. 7, 1649–1661.

- [4] R. M. Anderson and R. M. May, *Complex dynamical behavior in the interaction between HIV and the immune system*, in: *Cell to Cell Signalling: From experiments to theoretical models*, 335–349, Elsevier Ltd., Academic Press, 1989.
- [5] B. E. L. Boukari and N. Yousfi, *A delay differential equation model of HIV infection, with therapy and CTL response*, Bull. Math. Sci. Appl. **9** (2014), 53–68.
- [6] F. Brauer and C. Castillo-Chavez, *Mathematical Models in Population Biology and Epidemiology*, Second edition, Texts in Applied Mathematics **40**, Springer, New York, 2012.
- [7] B. Buonomo and C. Vargas-De-León, *Global stability for an HIV-1 infection model including an eclipse stage of infected cells*, J. Math. Anal. Appl. **385** (2012), no. 2, 709–720.
- [8] S. Butler, D. Kirschner and S. Lenhart, *Optimal control of chemotherapy affecting the infectivity of HIV*, in: *Advances in Mathematical Population Dynamics: Molecules, Cells and Man*, 104–120, World Scientific, Singapore, 1998.
- [9] P. van den Driessche and J. Watmough, *Reproduction numbers and sub-threshold endemic equilibria for compartmental models of disease transmission*, Math. Biosci. **180** (2002), no. 1-2, 29–48.
- [10] A. M. Elaiw, A. A. Raezah and K. Hattaf, *Stability of HIV-1 infection with saturated virus-target and infected-target incidences and CTL immune response*, Int. J. Biomath. **10** (2017), no. 5, 1750070, 29 pp.
- [11] P. Essunger and A. S. Perelson, *Modeling HIV infection of CD4⁺ T-cell subpopulations*, J. Theor. Biol. **170** (1994), no. 4, 367–391.
- [12] K. R. Fister, S. Lenhart and J. S. McNally, *Optimizing chemotherapy in an HIV model*, Electron. J. Differential Equations **1998**, No. 32, 12 pp.
- [13] T. R. Fouts, K. Bagley, I. J. Prado, K. L. Bobb, J. A. Schwartz, R. Xu, R. J. Zagursky, M. A. Egan, J. H. Eldridge, C. C. LaBranche, D. C. Montefiori, H. L. Buane, D. Zagury, R. Pal, G. N. Pavlakis, B. K. Felber, G. Franchini, S. Gordon, M. Vaccari, G. K. Lewis, A. L. DeVico and R. C. Gallo, *Balance of cellular and humoral immunity determines the level of protection by HIV vaccines in rhesus macaque models of HIV infection*, Proc. Natl. Acad. Sci. USA **112** (2015), no. 9, E992–E999.
- [14] R. C. Gallo, *A reflection on HIV/AIDS research after 25 years*, Retrovirology **3** (2006), no. 1, 7 pp.

- [15] G. P. Garnett, *An introduction to mathematical models in sexually transmitted disease epidemiology*, Sex. Transm. Infect. **78** (2002), no. 1, 7–12.
- [16] K. Hattaf and N. Yousfi, *Two optimal treatments of HIV infection model*, World J. Model. Simul. **8** (2012), no. 1, 27–35.
- [17] J. A. P. Heesterbeek and K. Dietz, *The concept of R_0 in epidemic theory*, Statist. Neerlandica **50** (1996), no. 1, 89–110.
- [18] G. Huang, Y. Takeuchi and W. Ma, *Lyapunov functionals for delay differential equations model of viral infections*, SIAM J. Appl. Math. **70** (2010), no. 7, 2693–2708.
- [19] D. Kamboj and M. D. Sharma, *Effects of combined drug therapy on HIV-1 infection dynamics*, Int. J. Biomath. **9** (2016), no. 5, 1650065, 23 pp.
- [20] R. Kaminski, R. Bella, C. Yin, J. Otte, P. Ferrante, H. E. Gendelman, H. Li, R. Booze, J. Gordon, W. Hu and K. Khalili, *Excision of HIV-1 DNA by gene editing: a proof-of-concept in vivo study*, Gene Ther. **23** (2016), no. 8-9, 690–695.
- [21] D. E. Kirschner and G. F. Webb, *A mathematical model of combined drug therapy of HIV infection*, Comput. Math. Methods Med. **1** (1997), no. 1, 25–34.
- [22] P. De Leenheer and H. L. Smith, *Virus dynamics: a global analysis*, SIAM J. Appl. Math. **63** (2003), no. 4, 1313–1327.
- [23] J. Lin, R. Xu and X. Tian, *Threshold dynamics of an HIV-1 model with both viral and cellular infections, cell-mediated and humoral immune responses*, Math. Biosci. Eng. **16** (2019), no. 1, 292–319.
- [24] M. Markowitz, M. Saag, W. G. Powderly, A. M. Hurley, A. Hsu, J. M. Valdes, D. Henry, F. Sattler, A. L. Marca, J. M. Leonard and D. D. Ho, *A preliminary study of ritonavir, an inhibitor of HIV-1 protease, to treat HIV-1 infection*, N. Engl. J. Med. **333** (1995), no. 23, 1534–1540.
- [25] N. Martin and Q. Sattentau, *Cell-to-cell HIV-1 spread and its implications for immune evasion*, Curr. Opin. HIV AIDS **4** (2009), no. 2, 143–149.
- [26] S. J. Merrill, *AIDS: background and the dynamics of the decline of immunocompetence*, in: *Theoretical Immunology, Part Two*, 59–75, New Mexico, 1987.
- [27] M. A. Nowak and C. R. Bangham, *Population dynamics of immune responses to persistent viruses*, Science **272** (1996), no. 5258, 74–79.

- [28] A. S. Perelson, *Modeling the interaction of the immune system with HIV*, in: *Mathematical and Statistical Approaches to AIDS Epidemiology*, 350–370, Lecture Notes in Biomath. **83**, Springer, Berlin, 1989.
- [29] A. S. Perelson, P. Essunger, Y. Cao, M. Vesanen, A. Hurley, K. Saksela, M. Markowitz and D. D. Ho, *Decay characteristics of HIV-1-infected compartments during combination therapy*, *Nature* **387** (1997), no. 6629, 188–191.
- [30] A. S. Perelson, D. E. Kirschner and R. De Boer, *Dynamics of HIV infection of CD4⁺ T cells*, *Math. Biosci.* **114** (1993), no. 1, 81–125.
- [31] A. Sigal, J. T. Kim, A. B. Balazs, E. Dekel, A. Mayo, R. Milo and D. Baltimore, *Cell-to-cell spread of HIV permits ongoing replication despite antiretroviral therapy*, *Nature* **477** (2011), no. 7362, 95–98.
- [32] Y. Tabit, K. Hattaf and N. Yousfi, *Dynamics of an HIV pathogenesis model with CTL immune response and two saturated rates*, *World J. Model. Simul.* **10** (2014), no. 3, 215–223.
- [33] Y. Tabit, A. Meskaf and K. Allali, *Mathematical analysis of HIV model with two saturated rates, CTL and antibody responses*, *World J. Model. Simul.* **12** (2016), no. 2, 137–146.
- [34] J. Wang, M. Guo, X. Liu and Z. Zhao, *Threshold dynamics of HIV-1 virus model with cell-to-cell transmission, cell-mediated immune responses and distributed delay*, *Appl. Math. Comput.* **291** (2016), 149–161.
- [35] X. Wang and W. Wang, *An HIV infection model based on a vectored immunoprophylaxis experiment*, *J. Theoret. Biol.* **313** (2012), 127–135.
- [36] Y. Wang, Y. Zhou, F. Brauer and J. M. Heffernan, *Viral dynamics model with CTL immune response incorporating antiretroviral therapy*, *J. Math. Biol.* **67** (2013), no. 4, 901–934.
- [37] D. Wodarz and D. H. Hamer, *Infection dynamics in HIV-specific CD4 T cells: Does a CD4 T cell boost benefit the host or the virus?*, *Math. Biosci.* **209** (2007), no. 1, 14–29.
- [38] H. Wu and A. A. Ding, *Population HIV-1 dynamics in vivo: applicable models and inferential tools for virological data from AIDS clinical trials*, *Biometrics* **55** (1999), no. 2, 410–418.

- [39] R. Xu, *Global stability of an HIV-1 infection model with saturation infection and intracellular delay*, J. Math. Anal. Appl. **375** (2011), no. 1, 75–81.
- [40] Y. Yan and W. Wang, *Global stability of a five-dimensional model with immune responses and delay*, Discrete Contin. Dyn. Syst. Ser. B **17** (2012), no. 1, 401–416.
- [41] J. Yang, X. Wang and F. Zhang, *A differential equation model of HIV infection of $CD4^+$ T-cells with delay*, Discrete Dyn. Nat. Soc. **2008**, Art. ID 903678, 16 pp.
- [42] J. A. Zack, S. J. Arrigo, S. R. Weitsman, A. S. Go, A. Haislip and I. S. Chen, *HIV-1 entry into quiescent primary lymphocytes: Molecular analysis reveals a labile, latent viral structure*, Cell **61** (1990), no. 2, 213–222.
- [43] J. A. Zack, A. M. Haislip, P. Krogstad and I. S. Chen, *Incompletely reverse-transcribed human immunodeficiency virus type 1 genomes in quiescent cells can function as intermediates in the retroviral life cycle*, J. Virol. **66** (1992), no. 3, 1717–1725.

Najmeh Akbari and Rasoul Asheghi

Department of Mathematical Sciences, Isfahan University of Technology, Iran

E-mail addresses: najmeh.akbari@math.iut.ac.ir, r.asheghi@iut.ac.ir

Maryam Nasirian

Epidemiology and Biostatistics Department, Health School, and Infectious Diseases and Tropical Medicine Research Center, Isfahan University of Medical Sciences, Iran

E-mail address: maryamnasirian17@gmail.com